

Verification of FEM modelling of composite materials based on the results of static strength test

Weryfikacja modelowania MES materiałów kompozytowych na podstawie wyników statycznej próby wytrzymałościowej

KATARZYNA GOJNY*

DOI: <https://doi.org/10.17814/mechanik.2019.2.23>

The article presents the verification of FEM modelling of composite materials based on the results of static strength test. The aim of the work was to examine whether the applied modelling of composite materials is correct and verify it with finite element method (FEM). The composite structure of the PW-6U glider was used as a model. In the program the numerical model (geometry and finite element mesh) of the glider's wing was created. The wing is made of glass fabrics and a spar with flanges with a glass roving. The composite structure of the wing, including composition, layout and thickness of laminate layers, fiber arrangement was exactly modelled in the program and then subjected to loads. Having the measurements from the static strength tests of the glider, the numerical results were compared with the experimental results.

Thanks to the applied modelling, the obtained numerical results were satisfactory and very close to the experimental results from the structural static tests of the glider. Therefore, it can be concluded that the conducted verification of FEM modelling of composite materials is correct.

Nowadays application of composite materials is increasingly expanding. Therefore, the modelling of composites becomes a significant issue. FEM modeling allows verification of the structure. At the stage of modelling modifications can be implemented and thus time and costs associated with subsequent changes in the production process may be saved. This is a very good solution which already at the design stage of the structure allows examination of its strength.

KEYWORDS: composite material, laminate, modelling, finite element method (FEM)

Artykuł prezentuje weryfikację modelowania MES materiałów kompozytowych na podstawie wyników statycznej próby wytrzymałościowej. Celem pracy było zbadanie, czy zastosowane modelowanie kompozytów jest prawidłowe, i zweryfikowanie tego metodą elementów skończonych (MES). Jako modelu użyto konstrukcji kompozytowego szybowca PW-6U. W programie wykonano model obliczeniowy (geometrię oraz siatkę elementów skończonych) skrzydła szybowca. Skrzydło jest zbudowane ze szklanych tkanin oraz dźwigara z pasami z włókna szklanego. Kompozytową strukturę skrzydła, opisaną m.in. przez rozmieszczenie, układ i grubość warstw oraz ułożenie włókien, dokładnie zamodelowano w programie, a następnie poddano obciążeniom. Na podstawie pomiarów ze statycznych prób wytrzymałościowych szybowca porównano wyniki numeryczne z wynikami eksperymentalnymi.

Dzięki zastosowanemu modelowaniu uzyskano zadowalające wyniki numeryczne, bardzo zbliżone do wyników eksperymentalnych z prób statycznych szybowca. Dlatego można stwierdzić, że przeprowadzona weryfikacja modelowania MES materiałów kompozytowych jest prawidłowa.

W dzisiejszych czasach zastosowanie materiałów kompozytowych coraz bardziej się rozszerza. Dlatego modelowanie kompozytów staje się istotnym zagadnieniem. Modelowanie metodą elementów skończonych pozwala na weryfikację konstrukcji. Na etapie modelowania można dokonać jeszcze ewentualnych modyfikacji i tym samym zaoszczędzić czas oraz ograniczyć późniejsze koszty związane ze zmianami w procesie produkcji. Jest to bardzo dobre rozwiązanie, które już w fazie projektowania konstrukcji pozwala na zbadanie jej wytrzymałości.

SŁOWA KLUCZOWE: materiały kompozytowe, laminat, modelowanie, metoda elementów skończonych (MES)

Sandwich and new generation aerospace composites

Composite materials have been used for thousands of years by people. The good example is plywood. In the 60s of the XX century the breakthrough was the invention of development of carbon and boron fibers [1]. Nowadays composite materials are increasingly being used in various fields of technology. Composites are utilized as structural materials, among others, in aviation in aircraft components and in astronautics in artificial satellites components. Thanks to their properties, they are also used in construction, stomatology, automotive industry and in the production of sport equipment. Their application is expanding steadily.

There are two main advantages which distinguish composite materials from other materials: improved strength and stiffness. Additional benefit is a unit weight basis. Composite materials are much lighter than other materials e.g. aluminium. One of the most commonly used laminates is sandwich composite (Fig. 1). Sandwich-structured composite consists of facings called skins and a core [2]. The skin materials are widely made of glass or carbon fiber reinforced plastics (GFRP or CFRP). Such fiber reinforced plastics are characterized by high specific modulus, strength and corrosion resistance. They may be fabricated in the form of unidirectional or woven laminae. The metal or aluminium alloys sheets may also constitute the skins. Although aluminium has high specific modulus, it is subject to denting and corrodes without treatment. The combination of different materials that are bonded to each other and also the stacking sequence determine the

* Mgr inż. Katarzyna Gojny (kgojny@meil.pw.edu.pl) – Division of Strength of Materials and Structures, Institute of Aeronautics and Applied Mechanics, Faculty of Power and Aeronautical Engineering, Warsaw University of Technology

stresses and strains in the laminate. The core materials are made of foam, honeycomb and balsa wood. The main feature of foam is its low density while balsa wood possesses high compressive strength. Honeycomb structures have different strength and stiffness properties depending on the material, cell size and thickness of the core. The skins are strong and stiff while the core is a lightweight but thick material. In addition, an important element of the sandwich composite is an adhesive in the form of film, paste or liquid which determines the integrity of the entire structure.

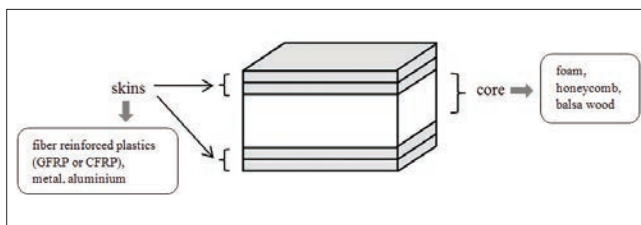


Fig. 1. Sandwich composite (own elaboration based on [2])

The rising use of composite materials can be found in the Boeing airplanes [3]. Early Boeing 747 aircraft has considerable amount of fiberglass sandwich in secondary structural applications which represents 1% of the structural weight. Furthermore, the flight control components of the Boeing 757 and 767 aircraft are made of carbon sandwich which corresponds to 3% of aircraft structural weight. In the Boeing 777 mainly the carbon fibers in a toughened epoxy matrix can be found in the empennage. These composite components constitute 11% of aircraft structural weight.

Hybrid composites are becoming more and more popular. Hybrid composite materials refer to composites in which a combination of distinct reinforced fibers appears. Subsequent layers of hybrid composite consist of different types of fabrics i.e. glass, carbon or aramid fabrics [4]. The combination of different fibers allows the advantages of individual fibers to be used. The main reason for utilizing such composites is an increase of stiffness. For example, a hybrid of glass and carbon was used in the wing-to-body fairings in Boeing 777 airplane [5].

New generation composite material is GLARE (Glass Laminates REinforced) which is a fiber metal laminate (FML) used in aerospace applications for skin elements. GLARE consists of thin aluminium sheets bonded together with adhesive containing embedded fibers [6]. The main advantage of this material is high resistance against fatigue. GLARE is used in fuselage skins in Airbus 380 airplane [7] and represents 3% of basic aircraft structural weight [8]. It results in fatigue and impact properties improvement maintaining lower density than commonly used materials. Moreover, in the A380 aircraft the carbon fiber reinforced plastics (CFRP) are mostly utilized which constitute 22% of aircraft structural weight [8].

The aeronautical design which takes advantage of composite materials is the new generation commercial the Boeing 787 Dreamliner aircraft. Its structure is composed of carbon fiber materials including such elements as wings, stabilizers and fuselage. The composite materials constitute 50% of aircraft structural weight [3]. The Airbus company has invested in the composite materials and the Airbus A350 has 53% CFRP content applied to the high-performance wing [9].

Composite materials are not only used in the commercial passenger air transport. They are also applied to

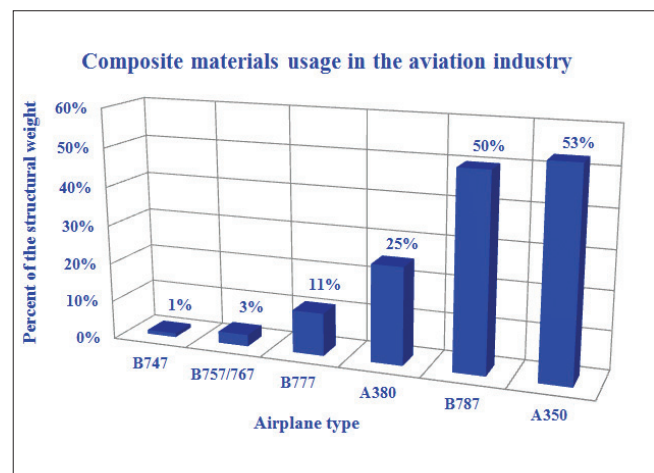


Fig. 2. Increased use of composites in the commercial airplanes (own elaboration based on [3, 8, 9])

gliders. For example, the sandwich composite including glass fiber reinforced plastics (GFRP) is used in the single seater PW-5 sailplane [10] and the dual seater PW-6 sailplane [11].

Composites are widely used in aerospace industry because of the light and stiff structure with high strength properties. Fig. 2 presents the increased use of composite materials in the commercial airplanes comparing to their structural weight. Thanks to a proper material design a balance in cost and performance can be achieved. A number of laminate compositions are under investigation, such as glass, carbon, aramid fibers with a variety of metal layers. However, the predictions of composite material properties and their optimal design can be obtained using numerical modelling described below.

Modelling of composite structures

Contemporary computational analyses of composite structures are performed using numerical methods. These methods allow predictions of composite material properties and behaviour. Prior to production of composite structures a process called modelling takes place that allows testing their strength. The special software gives the possibility of modelling of composite materials e.g. in the form of laminates.

However, it should be noted that the composite material is nonhomogeneous material with properties depending on the direction. Mathematical models of composites are much more complex than models of homogeneous and isotropic materials [4]. Stresses and strains analysis of the composite model can be conducted both in a micro scale and in a macro scale.

One of the common methods used for the structural analysis is the finite element method (FEM). The structure is divided into small elements called finite elements which constitute the mesh. In this method the approximations of the solution over each element in terms of nodal values are searched [12]. The discretized model is properly fixed and then subjected to loads. The primary results in the form of displacements, stresses and strains can be obtained. This method is a leading one used to design and analyze the aircraft components.

Due to the fact that stiffness plays a significant role in ensuring integrity and functionality of the aircraft structure, it is important to examine it. The stiffness can be understood as the ability to resist deformation. It depends on the material properties and the design configuration as well

as the way of loads application [13]. It can be checked using the numerical methods by computing and visualizing the displacements. The stiffness is a vital parameter especially for the composite materials and numerical software allows exploring it.

When modelling the composite materials it is important to apply a proper procedure in the selection of the finite elements which reflect anisotropic or orthotropic and laminated nature of the composite structures and also their stiffness and strength [14]. For the laminate, 2-dimensional shell elements or 3-dimensional solid elements can be used. The common choice is the shell element especially for the layered composite. Using one solid element for the multi-layered composite is impractical because it is expensive to run. Moreover, it leads to ill-conditioned sets of equations when stacking solid elements through the thickness of relatively thin plate [14]. Thus, the solid elements should be used for the composite of very thick lay-up or for more solid geometry than plate.

For aerospace applications it can be noticed that the shell elements are common choices for the wing skin, spar and rib models made of the layered composite materials [15–18]. FEM software can be used for the structural analysis of, for example, the composite wing made of woven carbon epoxy of unmanned aerial vehicle (UAV) [15]. In order to reduce the calculation time the numerical analysis can be performed only for one-half wing span due to symmetric geometrical structure. Subsequent iterations can be computed in order to find a better structural configuration. The final design may require changes in material, ply orientation or thickening. Another example of aircraft component which is subjected to finite element analysis can be part of the wing leading edge made of GLARE laminates [16]. Moreover, small segments of the aircraft wing as carbon fiber reinforced composite wing panels can be analyzed using FEM [17]. The finite element analysis (FEA) can be also conducted for the optimization process e.g. of laminated carbon fiber composite wing panels consisting of skin, ribs and stiffeners [18].

To conclude, modelling allows verification of the design and construction assumptions. It can be confirmed that the shell elements are reasonable for the laminates. In addition, the proper selection of the finite elements is important because of the material's choice. Moreover, one of the most important parameters is the mesh. The mesh should be designed in such a way to obtain acceptable accurate results but not with a long calculation time.

The aim of the research work

The aim of the work is to verify the applied FEM modelling of the composite materials. The object of the research is the wing of the PW-6U glider. The wing is composed of upper and bottom skin made of glass fabrics and spar flanges with a glass roving. The composition, layout and thickness of laminates and fiber arrangement were exactly modelled in the program and then subjected to loads. The obtained numerical results were compared to the experimental data obtained from the measurements during real static strength tests of the glider.

The software used in the research work is MSC Patran for pre/post-processing process and the solver MSC Nastran which uses the calculation FEM method. This method allows testing the strength of the structure. Different simulations (e.g. linear static) can be conducted. The displacements, deformations and stresses can be obtained as results.

Description of experimental results

The object of the research work was the left wing of PW-6U glider. The PW-6U is a dual-seat glider composed of epoxy-glass composite structure [11]. The wings have trapezoid contour ending with bow-shaped tips. The wings consist of mono-spar structures with sandwich shells. The basic dimensions of this glider's wing are presented in Table I.

TABLE I. PW-6U glider's wing dimensions [11]

Dimension	Value, mm
Wing length	7660
Root chord	1300
Tip chord	250

The experimental results constitute the measurements from the static strength tests of the glider's wing which were conducted for point A of the flight load envelope [19]. The glider's fuselage with both wings was fixed to the floor through beams system at two points and was inclined to the horizon at 12 degrees. Both wings were pulled up by electric spinning wheels using individual beam systems. Due to insufficient space in the laboratory room the right wing was shortened by approximately 1 meter. Therefore, the load beam systems of the right wing were modified in order to maintain the magnitude and location of the resultant force as well as load course along wingspan near the fuselage. Fig. 3 presents the experimental stand.



Fig. 3 Static strength test stand (author: Wojciech Frączek)

Two separate static strength tests were conducted. During these tests the measurements were done only for the selected points. The maximum vertical displacements of the left wing tip were registered for the 100% of load during two attempts [20].

TABLE II. Static strength tests measurements [20]

Test number	Maximum vertical displacement of the wing tip, mm
1	1438
2	1544

Numerical model

■ **Numerical model components.** MSC Patran/Nastran software was used for designing the numerical model and FEM computations. The numerical model of the PW-6U glider's wing was created in the MSC Patran (Fig. 4) based on the technical documentation [11]. The following wing components were modelled: upper and bottom wing skin, main spar, wing bayonet, wing tip rib, wing root rib, rear reinforced wall, aerodynamic air brake box, aileron wall, ribs closing the aileron section, rear fitting and sleeves in the bayonet holes. The global coordinate system is right-handed and is indicated by the cross mark in Fig. 4. The global X axis is along longitudinal axis of symmetry of the glider while the global Y axis is collinear with the leading edge of the wing. The global coordinate system is placed at the half of the width of the glider's fuselage.

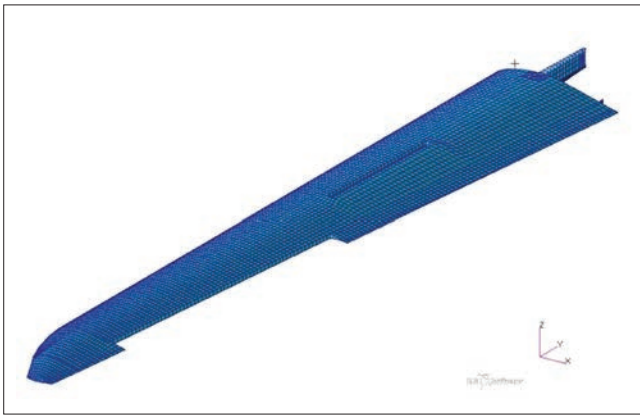


Fig. 4. Numerical model of the wing (own elaboration)

Nastran has an extensive library of finite elements which cover a wide range of physical behaviour. In the model different types of finite elements were used: bar-type elements (BAR2), shell-type elements (QUAD4), hexagonal-type elements (HEX8). Table III shows the types of finite elements which were used for modelling the wing components. The dimension of QUAD finite element along the wingspan was set to 50 mm. Table IV presents the number of finite elements which were used in the model depending on the type of the finite element.

TABLE III. Types of finite elements used in the wing model

Component of the wing	Type of finite element
Upper and bottom wing skin	Quad4
Main spar: <ul style="list-style-type: none"> • laminar wall • spar flanges • reinforced crossbars 	Quad4 Bar2 Bar2
Wing bayonet: <ul style="list-style-type: none"> • skin • core • spar flanges 	Quad4 Hex8 Hex8
Wing tip and root ribs, ribs closing the aileron section	Quad4
Rear reinforced wall, aileron wall	Quad4
Aerodynamic air brake box and its reinforced crossbars	Quad4 Bar2
Rear fitting and sleeves	Quad4

TABLE IV. Number of finite elements used in the model

Type of finite element	Number of finite elements used in the model
Quad4	9645
Bar2	515
Hex8	346
Total number of finite elements: 10 506	
Total number of nodes: 9823	

Fig. 5 shows the wing components near the fuselage i.e. wing root rib, main spar, wing bayonet, rear reinforced wall and rear fitting. The bayonet's holes with the sleeves were also modelled. For the bayonet various types of the finite elements were used depending on the wing bayonet's component (Table III).

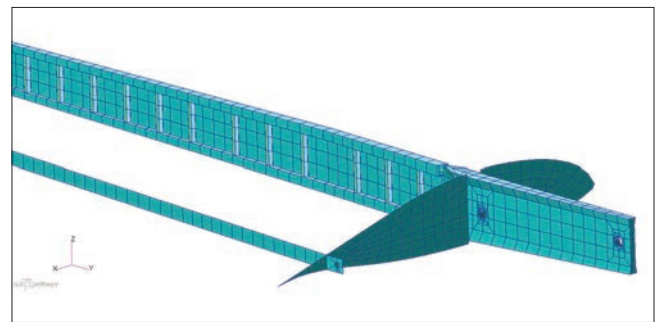


Fig. 5. Wing numerical model components (own elaboration)

Fig. 6 presents the photo of the part of the wing's main spar. It can be noticed that the spar is composed of vertical reinforced crossbars which were also modelled (Fig. 7) including their detailed cross-sections according to the glider's documentation [11]. Moreover, the cross-sections of the spar flanges change along the wingspan and their dimensions become smaller towards the wing tip. Such variable change of the spar flanges cross-sections was also modelled.



Fig. 6. Main spar with vertical reinforced crossbars (author: Katarzyna Gojny)

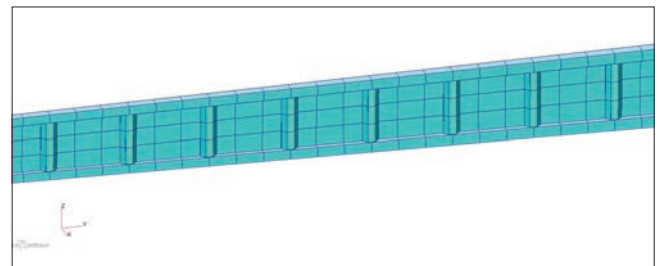


Fig. 7. Main spar model components (own elaboration)

The aerodynamic air brake box was modelled including the reinforced crossbars (Fig. 8). These crossbars are the vertical components which strengthen the structure. The cross-sections of these crossbars are different [11].

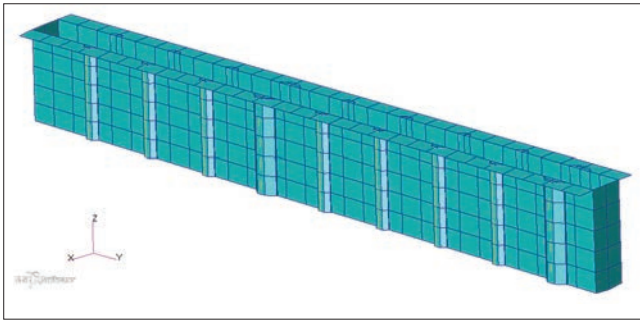


Fig. 8. Aerodynamic air brake numerical model (own elaboration)

Fig. 9 and Fig. 10 present the coupling between the wing skins and the main spar which was modelled applying the rigid elements called RBE2 elements. Such rigid elements do not require the associated property entry. The RBE2 elements are utilized for neighbouring elements which differ greatly in relative stiffness [21]. The RBE2 does not add any physical stiffness to the model and thus it does not result in numerical difficulties. In the wing model the RBE2 elements connect the shell structure of the skin and the structure of the main spar. The RBE2 acts like a constraint element that records the displacement relationship between two or more grid points.

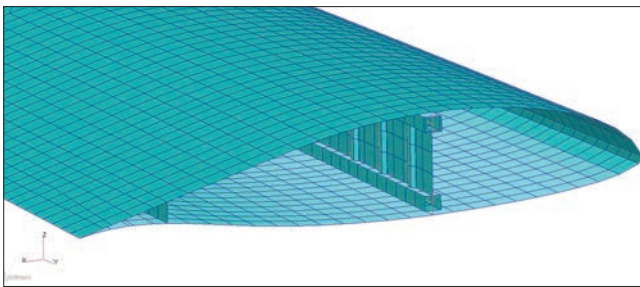


Fig. 9. The RBE2 element coupling (own elaboration)

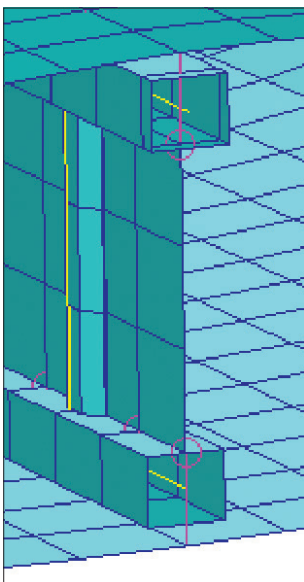


Fig. 10 The RBE2 coupling under magnification (own elaboration)

■ **Model loads and boundary conditions.** The loads were applied to the model based on the documentation of static strength tests [19]. The loads in the form of force vectors were attached to the model, at 24 nodes, from which they were transferred via rigid RBE3 elements to the nodes of the upper wing skin (Fig. 11). The RBE3 element is used for distributing the applied loads and it does not add additional stiffness to the modelled structure [21]. In the program such solution of applying the loads repre-

sents the beams systems used during real structural static tests. The loads are applied at leading edge locations and above main spar locations along wingspan.

The wing model was fixed at three locations: both holes in the bayonet and hole in the rear fitting. The bottom element edges of the inner bayonet's hole, the upper element edges of the outer bayonet's hole and all element edges of the rear fitting's hole were restrained. All element edges of above-mentioned holes were fixed in X, Y, Z translational directions.

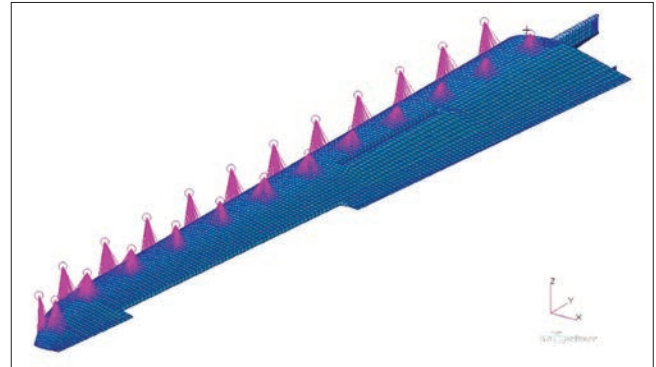


Fig. 11. Wing model loads (own elaboration)

Fig. 12 shows the force vector and RBE3 finite element under magnification. The forces were applied at angle 12 degrees inclined to the global vertical axis Z according to the program of the static strength tests [19]. The total load value was equal to 10 641 N while its vertical component along global Z axis was 2212,388 N and its horizontal component along X axis was 10 408,469 N.

During the real structural static test the beam systems were attached to the wing upper skin through the special patches bonded to the wing's surface. This way of transforming the loads into the structure is presented in Fig. 13. Fig. 14 shows the part of the wing with the modelled representation of above-mentioned patches as highlighted red shell elements. The RBE3 elements are attached to the nodes of upper wing skin in places of these patches.

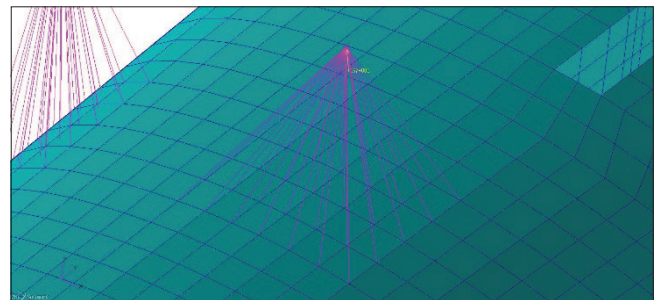


Fig. 12. Force vector attached to RBE3 element (own elaboration)



Fig. 13. Patches bonded to the wing's surface (author: Wojciech Frączek)

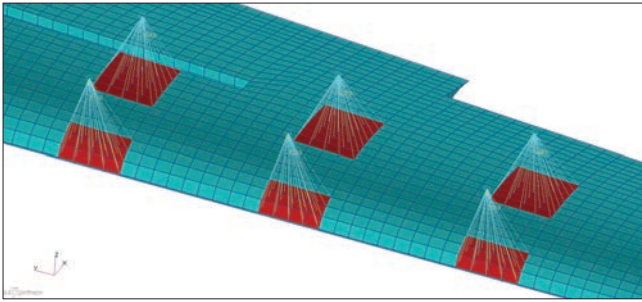


Fig. 14. Numerical representation of patches bonded to the wing's surface (own elaboration)

■ **Composite material data.** During the research work the main emphasis was put on the correct modelling of the composite structure. The upper and bottom wing skins are made of a sandwich-structured composite. Such composite is composed of layers of glass fabric reinforced plastic and foam. In the program the PCOMP material card was used to define the composite material laminate. The PCOMP material card includes: stacking sequence definition, material properties for each layer, thickness of a layer and orientation angle of fiber arrangement [21].

In different places of the wing skin the total thickness of laminate layers is variable. Fig. 15 shows the model of the upper wing skin with distinct colors representing areas with different thickness of laminate layers. The closer to the wing root rib (near the glider's fuselage), the thicker the composite becomes. Moreover, the leading and trailing edges of the wing are also reinforced because there are more layers of epoxy-glass composite in these places.

The main composite material used in the model was glass fiber reinforced plastic (GFRP) called Interglas. Table V presents the material from which the particular wing component is made. The material data including Young modulus, Kirchhoff modulus, Poisson ratio and densities are confidential and thus they are not presented in this paper.

Table VI presents the example of the detailed layout of sandwich-structured composite used in the model in the reinforced belts on both sides of the air brake box. This laminate is composed of two external skins, foam as a core, internal skin, belt and reinforcement. It can be noticed that the fibers orientation angle is not constant through the laminate. It has 45 degrees value for the skins and reinforcement layers but for the belt layer it is equal to 90 degrees.

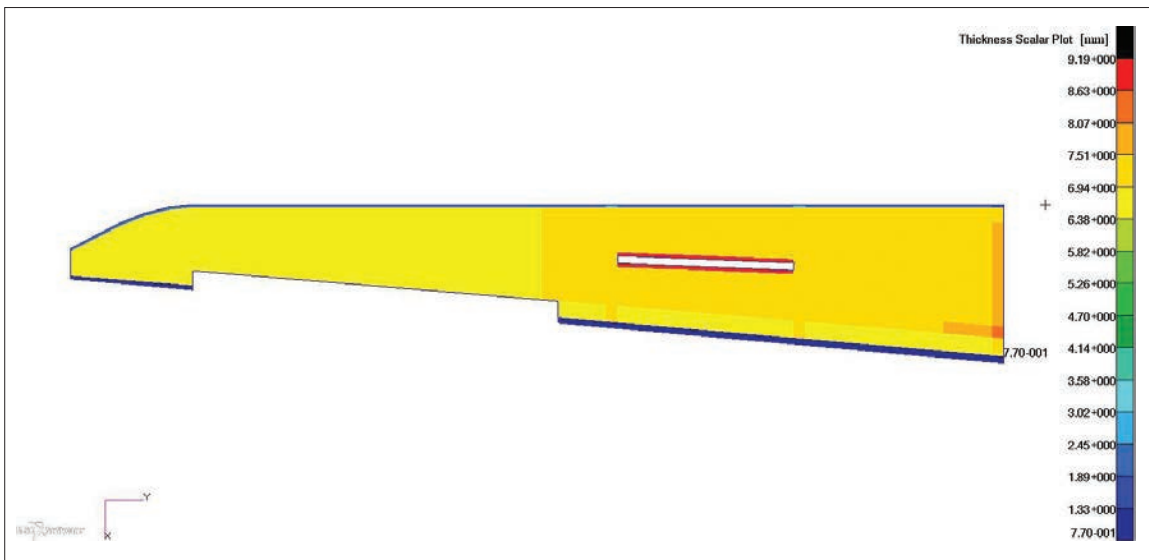


Fig. 15. Upper wing skin with areas of different thickness of laminate layers (own elaboration)

TABLE V. Types of materials used in the wing model

Component of the wing	Material
Upper and bottom wing skin	Interglas (GFRP) and foam
Main spar: <ul style="list-style-type: none"> laminar wall spar flanges reinforced crossbars 	Interglas (GFRP) Glass roving Interglas (GFRP)
Wing bayonet: <ul style="list-style-type: none"> skin core spar flanges 	Interglas (GFRP) Foam Glass roving
Wing tip and root ribs, ribs closing the aileron section	Interglas (GFRP)
Rear reinforced wall, aileron wall	Interglas (GFRP)
Aerodynamic air brake box and its reinforced crossbars	Interglas (GFRP) Interglas (GFRP)
Rear fitting and sleeves	Steel

TABLE VI. Example of sandwich-structured composite used in the wing model [11]

No.	Name of the layer	Material symbol	Thickness of the layer, mm	Fibers orientation angle, deg
1	External skin	Interglas (GFRP)	0,15	45
2	External skin	Interglas (GFRP)	0,36	45
3	Foam	Foam material	6	0
4	Internal skin	Interglas (GFRP)	0,26	45
5	Belt	Interglas (GFRP)	0,19	90
6	Reinforcement	Interglas (GFRP)	0,26	45

Comparison of numerical and experimental results

MSC Patran was used for pre-processing and post-processing. The MSC Nastran was used as a solver for the numerical computations. The linear static analysis was conducted in the numerical computations. The numerical results of the wing model displacements were obtained which are shown in Fig. 16. The wing model was deformed in a vertical plane in the upward direction. The maximum vertical displacement obtained for the left wing tip was equal to 1562 mm.

It must be emphasized that only two attempts of static strength tests were conducted and during both static strength tests the measurement was limited to the selected point which was the wing tip. During these two attempts the maximum vertical displacement of the wing tip was measured. Moreover, the displacement measurements obtained in both attempts differ by 106 millimeters. Therefore, it can be concluded that the measurement data were poor because also during structural static tests the wing deflection along wingspan was not recorded.

Table VII presents the comparison between maximum vertical displacements of the wing tip for both structural static tests and the numerical result. It can be noticed that the numerical result preserves the order of magnitude

of experimental results which is approximately equal to 1,5 meter.

TABLE VII. Comparison of experimental [20] and numerical results

Maximum vertical displacement of the wing tip, mm		
Static test No. 1	Static test No. 2	Numerical result
1438	1544	1562

The FEM software allows the display of displacements or stresses of the components of the model. It is a very useful tool allowing examination of the internal structure. Fig. 17 presents the displacements of the wing model components: main spar, wing bayonet, all ribs, aerodynamic air brake box, aileron and rear reinforced walls, rear fitting. Modelling of composite materials allows computation of interlaminar stresses with respect to the fibers direction. These stresses can be displayed for each layer of the laminate. The examples of the X stresses along 1st fibers direction for first laminate's layer for upper and bottom skin are presented in Fig. 18 and in Fig. 19 respectively. It can be noticed that the largest values of X stress appear at the bayonet and wing root rib connection in the plane of main spar.

Fig. 16. Numerical results of the wing model displacements in millimeters (own elaboration)

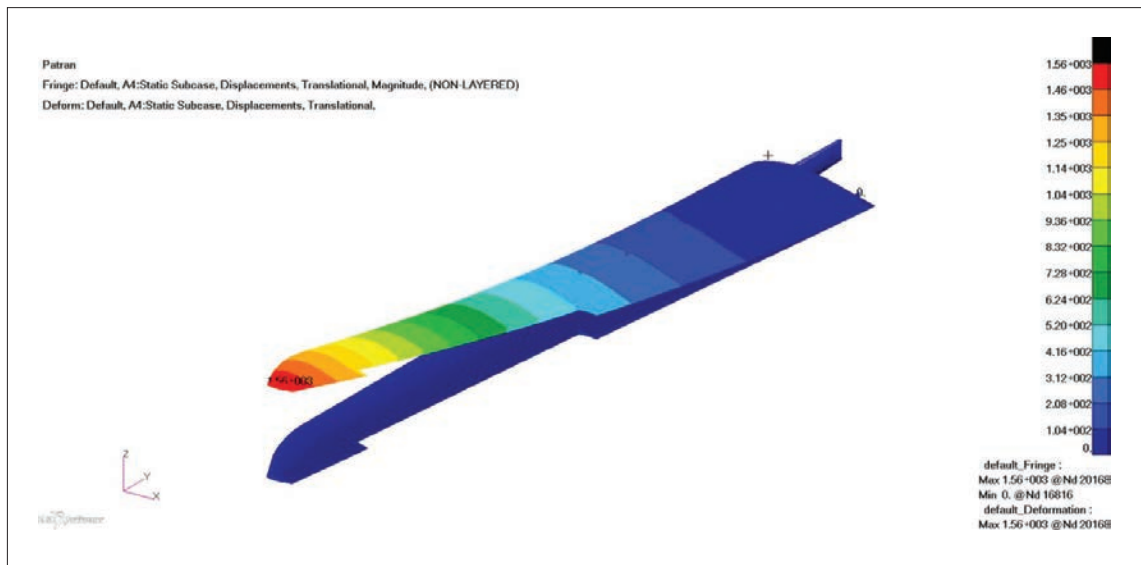
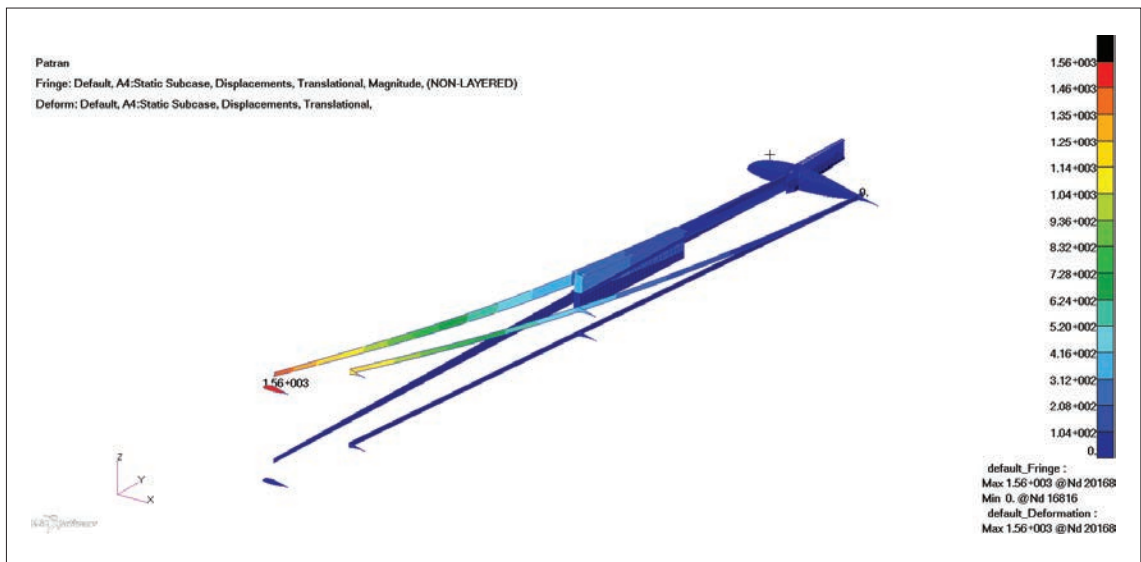


Fig. 17. Numerical results of the wing model components displacements in millimeters (own elaboration)



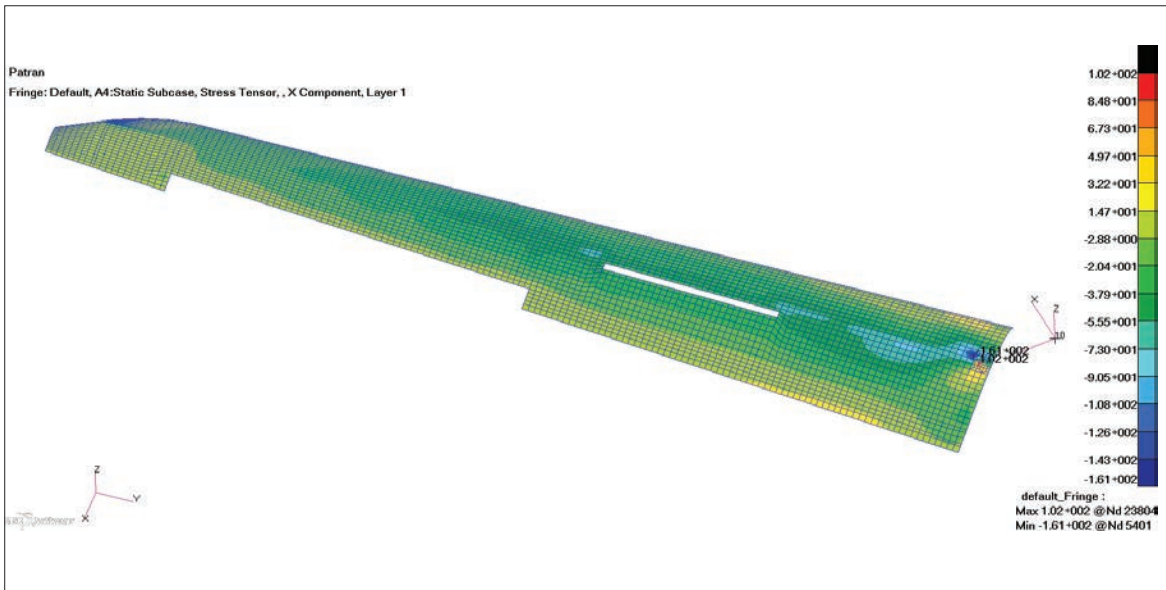


Fig. 18. Numerical results of X stress component along 1st fibers direction in MPa for upper skin (own elaboration)

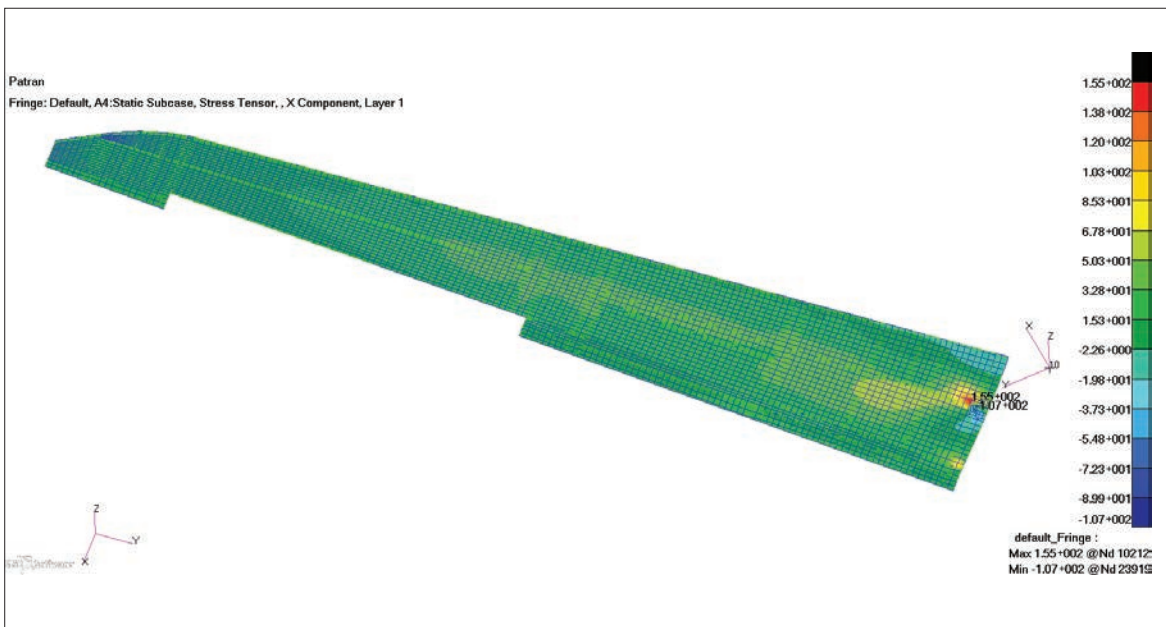


Fig. 19. Numerical results of X stress component along 1st fibers direction in MPa for bottom skin (own elaboration)

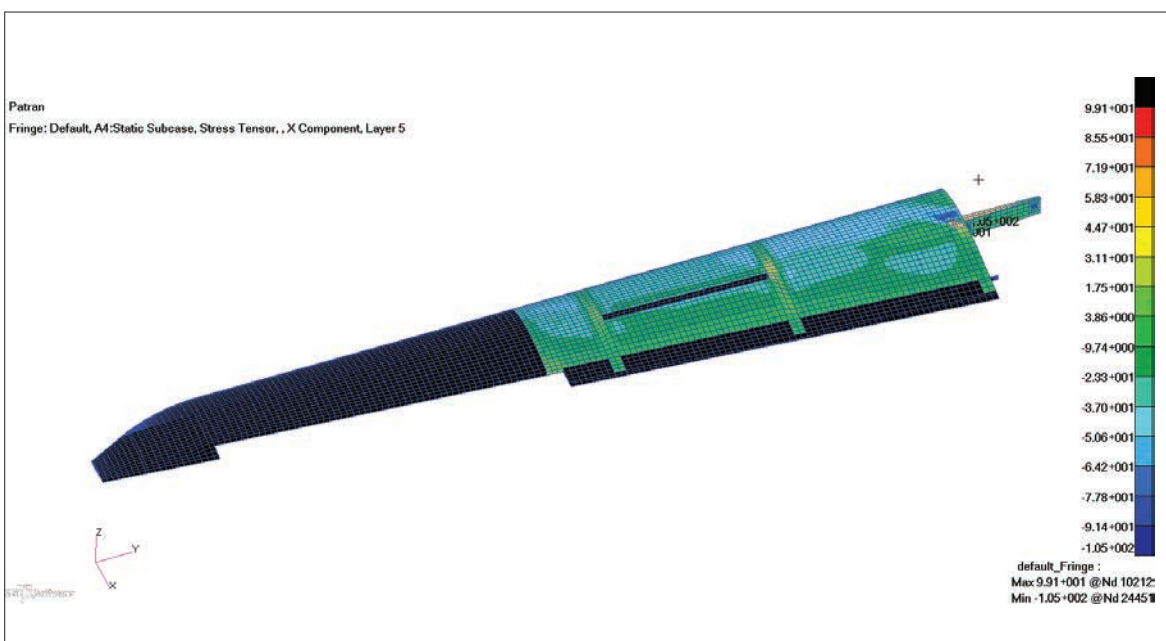


Fig. 20. Numerical results of X stress component along 1st fibers direction in MPa for 5th layer (own elaboration)

It is possible to display stresses for internal layers of the laminate. Thus, the program displays only numerical results for the finite elements which include the particular layer. Fig. 20 indicates the X stresses along 1st fibers direction for the fifth laminate's layer. The fifth layer was chosen as the example in order to show that not everywhere such layer exists in the wing model. For this fifth layer the largest stress concentration areas appear at the bayonet and wing root rib connection.

Conclusions

The finite element model of the PW-6u glider's wing was successfully created making it useful for the research. The wing composite structure was precisely modelled including composition, layout and thickness of laminate layers and fiber arrangement.

The applied modelling made it possible to obtain the satisfactory numerical results which were very close to the experimental results from the static strength tests of the glider. Thus, it can be concluded that such verification of FEM modelling of composite materials is correct. The aim of the research work was reached.

Moreover, if the verification of FEM modelled structure is correct, it can be expected that the modifications of the structure will reflect correctly the change of strength, stiffness, etc. Furthermore, in case of the composite materials the FEM software allows examination of interlaminar stresses for each layer of laminate. Such analysis may result in the safety assessment of the structure. Therefore, this numerical model of the PW-6U wing can be useful for further research work due to the fact that the advantages of composite materials are very compelling and their exploration and development are worth carrying out.

Nowadays application of composite materials is increasingly expanding. Therefore, the modelling of composites becomes a significant issue. FEM modelling allows verification of the structure. At the stage of modelling modifications can be implemented and thus time and costs associated with subsequent changes in the production process may be saved. This is a very good solution which already at the design stage of the structure allows examination of its strength.

REFERENCES

1. Kaczorowski M., Krzyńska A. „Konstrukcyjne materiały metalowe, ceramiczne i kompozytowe”. Warszawa: Oficyna Wydawnicza Politechniki Warszawskiej, 2017, pp. 271–275.
2. Kaw A.K. “*Mechanics of Composite Materials*”. 2nd Edition. Florida: CRC Press Taylor & Francis Group, 2006, pp. 34–38, 369–430.
3. Roeseler W.G., Sarh B., Kismarton M.U., The Boeing Company. “Composite structures: the first 100 years”. Kyoto: 16th International Conference on Composite Materials. 2007.
4. Boczkowska A., Krzesiński G. „Kompozyty i techniki ich wytworzenia”. Warszawa: Oficyna Wydawnicza Politechniki Warszawskiej, 2016, pp. 72–74, 153–154.
5. Jones R.M. “*Mechanics of Composite Materials*”. 2nd Edition. Philadelphia: Taylor & Francis, 1999, pp. 26–53.
6. Vlot A. “*Glare*”. Dordrecht: Kluwer Academic Publishers, 2001, pp. 1–2.
7. King D., Inderwildi O., Carey C. “Advanced aerospace materials: past, present and future”. *Aviation and the Environment*. 2009, pp. 22–27.
8. Oczko K.E. „Kompozyty włókniste – właściwości, zastosowanie, obróbka ubytkowa”. *Mechanik*. 7 (2008): pp. 578–582.
9. “World Airliner Directory, Special Report, Airbus A350”. *Flight International*. 188, 5515 (2015): pp. 32–33.
10. Doświadczalne Warsztaty Lotniczych Konstrukcji Kompozytowych Spółka z o.o. „Instrukcja użytkownika w locie szybowca B1-PW-5”. 2001.
11. Zespół Naukowo-Badawczy Lotniczych Konstrukcji Kompozytowych. „Dokumentacja techniczna szybowca PW-6U”. Warszawa: Politechnika Warszawska, Instytut Techniki Lotniczej i Mechaniki Stosowanej, 1996.
12. Reddy J.N. “*An Introduction to the Finite Element Method*”. 2nd Edition. United States of America: McGraw-Hill, Inc., 1993, pp. 5–6.
13. Wiśniowski W. „Sztwność i utrata sztywności konstrukcji lotniczych”. *Prace Instytutu Lotnictwa*. 214 (2011): pp. 15–23.
14. Matthews F.L., Davies G.A.O., Hitchings D., Soutis C. “*Finite Element Modelling of Composite Materials and Structures*”. Cambridge: Woodhead Publishing Limited, 2003, pp. 3–5, 71–93.
15. Rumayshah K.K., Prayoga A., Agoes Moelyadi M. “Design of High Altitude Long Endurance UAV: Structural Analysis of Composite Wing using Finite Element Method”. *Journal of Physics: Conference Series*. 5th International Seminar of Aerospace Science and Technology. 1005, 1 (2018): pp. 1–11.
16. Shetty B.P., Reddy S., Mishra R.K. “Finite Element Analysis of an Aircraft Wing Leading Edge Made of GLARE Material for Structural Integrity”. *Journal of Failure Analysis and Prevention*. 17, 5 (2017): pp. 948–954.
17. Splichal J., Pistek A., Hlinka J. “Dynamic tests of composite panels of aircraft wing”. *Progress in Aerospace Sciences*. 78 (2015): pp. 50–61.
18. Barkanov E., Ozoliņš O., Eglītis E., Almeida F., Bowering M.C., Watson G. “Optimal design of composite lateral wing upper covers. Part I: Linear buckling analysis”. *Aerospace Science and Technology*. 38 (2014): pp. 1–8.
19. Zespół Naukowo-Badawczy Lotniczych Konstrukcji Kompozytowych. „Program prób statycznych szybowca PW-6 (wersja użytkowa)”. Nr dokumentu PW-6/PPSU/1/99. Warszawa: Politechnika Warszawska, Instytut Techniki Lotniczej i Mechaniki Stosowanej, 1999.
20. Przedsiębiorstwo doświadczalno-produkcyjne szybownictwa. „Sprawozdanie z prób statycznych szybowca PW-6”. Nr dokumentu PW-6/SPS-U/1/99. Bielsko-Biala, 1999.
21. MSC Software Corporation. “*Linear Static Analysis User's Guide*”. 2018. ■